Canadian Chemical Transactions Year 2016 | Volume 4 | Issue 3 | Page 267-283

Research Article

DOI:10.13179/canchemtrans.2016.04.03.0302

Spectroscopic Studies of the Optical, Thermal and Morphological Properties of a Newly Synthesized Self-Assembled PTCDI

Andrea Sandra Christine D′Cruz and K.R. Sankaran*

Department of Chemistry, Annamalai University, Annamalainagar 608 002, India.

**Corresponding Author, Email profkrs15@gmail.com*

Received: *April 18, 2016* ***Revised:*** *June 15, 2016* ***Accepted:*** *June 16, 2016* ***Published:*** *June 27, 2016*

Abstract: In this paper, we have carried out the synthesis of a newly synthesized symmetrical PTCDI namely N,N′-Bis(3-butoxypropyl)perylene-3,4,9,10-tetracarboxylic diimide and is represented as BP-PTCDI respectively. Compound BP-PTCDI was characterized by using different spectroscopic measurements such as FT-IR, ^{1}H NMR, ^{13}C NMR, 2D NMR and mass spectral analysis. The optical properties at various concentrations were carried out by using UV-vis spectroscopy and fluorescene spectroscopy techniques. The absorption maximum for the synthesized compound was observed in the range 400-600 nm, whereas the emission spectrum was observed at approximately 525 nm. The self-assembly of the synthesized compound showed remarkable formation of aggregates due to π-π stacking. The aim of this work is to understand the optical properties as well as to determine the structure of the synthesized compound at the molecular level using theoretical studies such as NMR shielding, Mulliken charge transfer, molecular electrostatic potential (MEP) and natural bonding order (NBO) analysis.

Keywords: PTCDI; self-assembly; NMR shielding; mulliken charge transfer; MEP; NBO.

1. INTRODUCTION

Organic semiconductors are known to have fuelled a lot of interest spanning over three decades due to its low cost and ease of availability. n-type organic semiconductors are of prominent importance in the organic electronic industry. Among all the n-type organic semiconductors used, perylene tetracarboxylic diimides (PTCDIs) are known to be largely studied due to its good π-π stacking configuration. PTCDIs also show many other interesting properties such as good optical, thermal, photoluminescent and photophysical properties. They are also known to exhibit high yields of fluorescence and also show charge transport properties [1-8]. Besides, they are also known to exhibit excellent tinctorial strength and relative chemical inertness along with strong absorption in the visible region and also help facilitate good electron mobilities [9,10]. Another fascinating property of PTCDI derivatives is that they favour charge transfer due to large intermolecular coupling which may lead to the formation of charge transfer excitons [2].

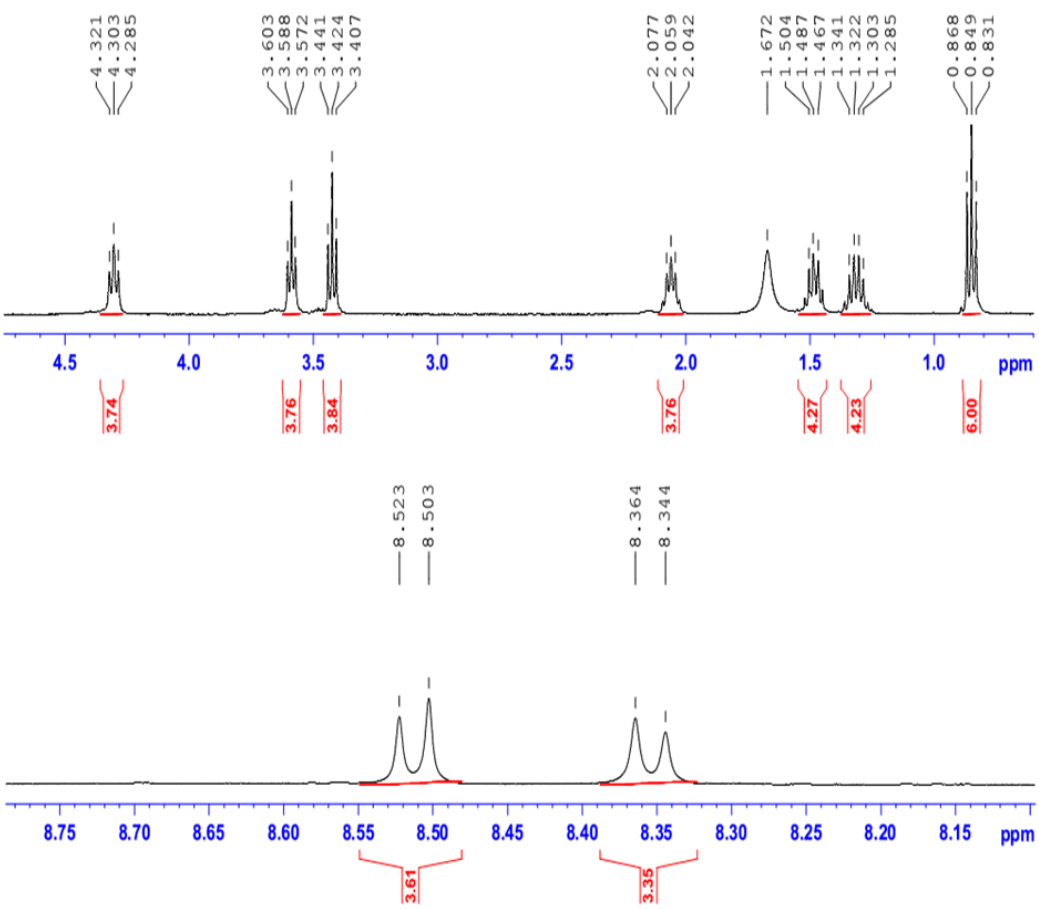

Figure 1. [1]H NMR spectra of BP-PTCDI

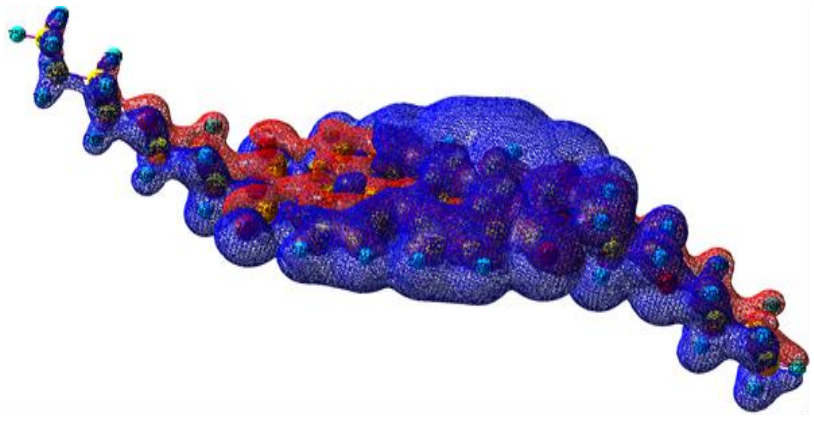

Figure 2. NMR shielding of BP-PTCDI

However, a major drawback with PTCDIs is their instability in air due to its low charge carrier motilities that arises due to weak intermolecular interactions and also because of its insolubility in most of

the organic solvents. Most organic materials are prone to degradation by exposure to oxygen and water vapour. Thermodynamic studies suggest that lower the LUMO energies are capable of demonstrating greater stability to an organic radical anion attack by water and oxygen, which has delivered a series of useful air-stable, n –type devices. Another serious drawback with n-type organic devices is stabilizing the radical anion during device operation. Many n-type organic devices develop large positive threshold voltage shifts and decreased mobility during operation which indicates the presence of trapped charge [2]. The transport of charges in organic layers is hence important in the design of organic electronics.

These drawbacks has driven many researchers and scientist alike to create novel, high performance, soluble n-channel materials for developing stable organic and opto-electronic devices by increasing the solubility of PTCDIs by modifying the structure of the two side chains at the two N-positions of the imide or substitution at the bay positions. Introduction of electron-withdrawing groups at either the ortho / bay-position shift the reduction potential of PTCDIs to more positive values which helps to increase the electron affinities [11]. Modification of the side chains do affect the conformation and strength of molecular stacking of PTCDI molecules when assembled into crystalline materials **[**12**]**. The choice of side chain substituents plays an important role in the solubility. Balakrishnan *et al*. in their work reported that the side chain substituents does have a strong impact on the morphological and electronic features of the synthesized compounds [13] It in turn also has a strong impact on the molecular packing of the compounds due to strong intermolecular interactions such as π-π stacking configurations.

Thus PTCDIs finds its way for applications in OFETs, fluorescent solar collectors, electro-photographic devices, dye lasers, organic photovoltaic cells (OPVs) and optical power limiters [14-19]. Another interesting feature of n- type PTCDIs is that their reversible n-type property makes them arguably suitable for organic electronic applications in electro-chromic and super capacitor devices [20].

The main objective of this work is the synthesis of a new PTCDI which will help to serve as useful applications in the organic electronic industry. Here in this paper, we present the synthesis, optical properties and the computational studies for the synthesized compound **BP-PTCDI** respectively.

2. MATERIALS AND METHODS

2.1 Materials used

Perylene-3,4,9,10-tetracarboxylic dianhydride, 3-butoxypropylamine and imidazole were purchased from Sigma Aldrich, India having a purity grade of 98%. All chemicals were used as such without any further purification.

2.2 Instrumentation

The Fourier transform- infra red (FT-IR) measurements were carried out in the regions ranging from 4000-400 cm^{-1} on a NICOLET AVATAR 360 instrument using KBr pellet. The ^{1}H NMR and ^{13}C NMR spectra in $CDCl_3$ were recorded on a BRUKER 400/100 MHz NMR spectrometer. All the chemical shifts were measured in parts per million (ppm). The UV–Vis spectra were recorded with UV-1650 PC double beam UV-Visible spectrophotometer. Emission spectra were measured using a Varian fluorescence spectrophotometer ((λ_{exci} = 460 nm). Mass spectra were recorded on a JEOL GCMATE 11

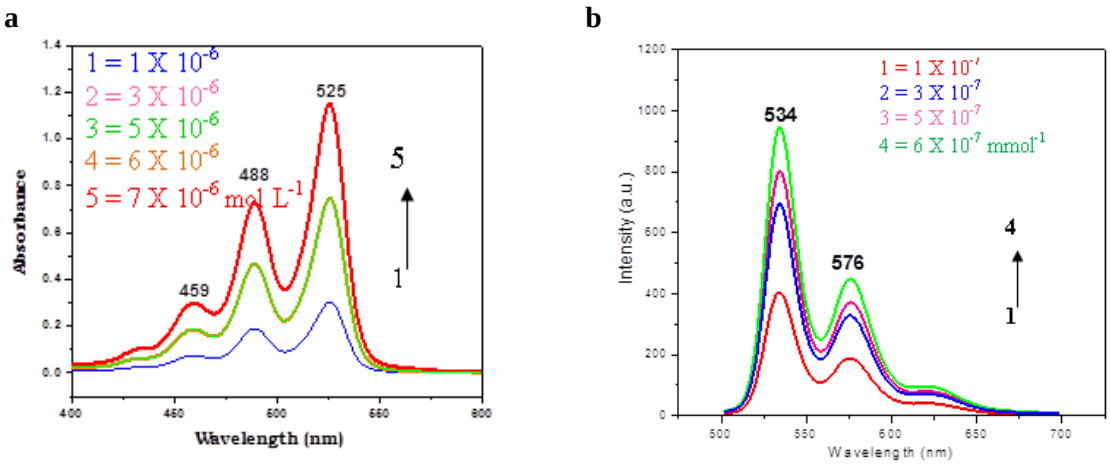

Figure 3. a) UV-vis spectra of BP-PTCDI in $CHCl_3$ b) Fluorescence spectra of BP-PTCDI in $CHCl_3$

GC Mass spectrometer. SEM image was recorded using a JEOL INDIA Pvt. Ltd., JSM-6610LV instrument. The sample was prepared by casting a drop of the self-assembly solution onto a clean glass slide, followed by annealing it in an oven for about half hour at 45°C. The sample was then coated with platinum prior to the SEM measurement. Fluorescence microscopic image was captured on a LEICA DM 2500 fluorescence micrsocope. Optical microscopic images were obtained using a MAGNIUS MLX model, MAGNIUS MICROSCOPE. Phase contrast microscopic images were obtained using a NIKON TYPE 120c, NIKON ECLIPSE TS 100 microscope. Differential scanning calorimetry was carried out on a NETZSCH STA 449F3 instrument. The sample was recorded upto 350°C and heated at 5 K min^{-1} in nitrogen.

2.3 Experimental section

The starting compound used is the commercially available perylene tetracarboxylic dianhydride (PTCDA). **BP-PTCDI** was synthesized by carrying out a condensation reaction of PTCDA (0.395 g, 1 mmol), imidazole (~6 g) and 3-butoxypropylamine (0.307 mL, 2 mmol)/ in a 50 mL round bottom flask for a period of 8-12 h at 140-160°. A nitrogen gas environment was developed for the reaction to proceed. The completion of the reaction was determined by carrying out thin layer chromatography (TLC) using suitable eluents such as hexane and ethyl acetate (3:2 ratios). The reaction mixture was then treated with 100 mL of ethanol and 300 mL of 2N HCl. The reaction mixture was left to stir overnight after which it was washed with copious amount of distilled water till the washings turned neutral. The synthesized compound was then purified by subjecting the red-maroon precipitate to a vigorous solvent wash (methanol) and dried again under normal atmospheric conditions. The dried compound was then used for further characterizations.

BP-PTCDI: ^{1}H NMR (400MHz, $CDCl_3$): δ 8.50-8.52 [(d, 4H, (H-4, H-7, H-11, H-14)], 8.34-8.36 [(d, 3H, (H-5, H-6, H-12, H-13)], 4.28-4.32 [(t, 4H, H-3′(3″)], 3.57-3.60 [(t, 4H, H-1′(1″)], 3.40-3.44 [(t, 4H, H-5′(5″)], 2.04-2.07 [(t, 4H, H-2′(2″)], 1.46-1.50 [(m, 4H, H-6′(6″)], 1.28-1.34 [(m, 4H, H-7′(7″)], 0.83-0.86 [(t, 6H, H-8′(8″)]; ^{13}C NMR (100 MHz, $CDCl_3$): δ 163.2 (C=O), 134.1-122.8 (perylene C), 70.7 [(C-5′(5″)], 68.8 [(C-1′(1″)], 38.4 [(C-3′(3″)], 31.8 [(C-6′(6″)], 28.2 [(C-2′(2″)], 19.3 [(C-7′(7″)], 13.9 [(C-

8′(8″)]; IR (KBr, cm^{-1}): υ 2958-2865(aliphatic C-H stretching), 1700 and 1661 (C=O stretching), 1348 (C-N stretching); Mass $C_{40}H_{42}N_2O_6$: 618.2 (calcd), 614.2 (found); UV-vis ($CHCl_3$): λ_{max} (nm) 459, 488, 525; fluorescence ($CHCl_3$): λ_{max} (nm) 534, 576 (λ_{exc}=460 nm); yield: 70%

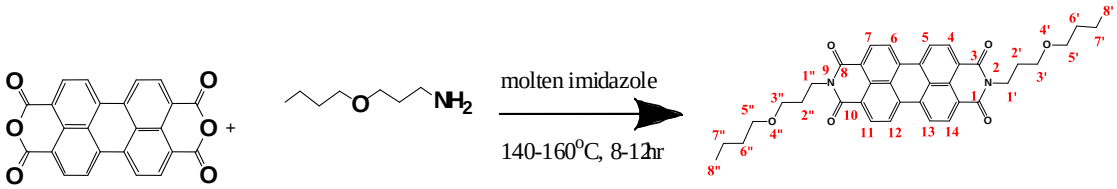

Scheme 1

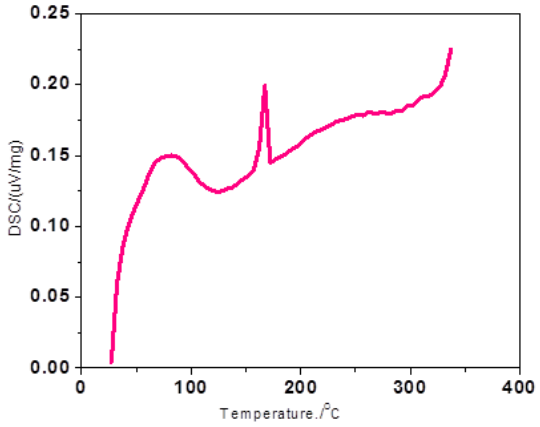

Figure 4. DSC thermogram of BP-PTCDI

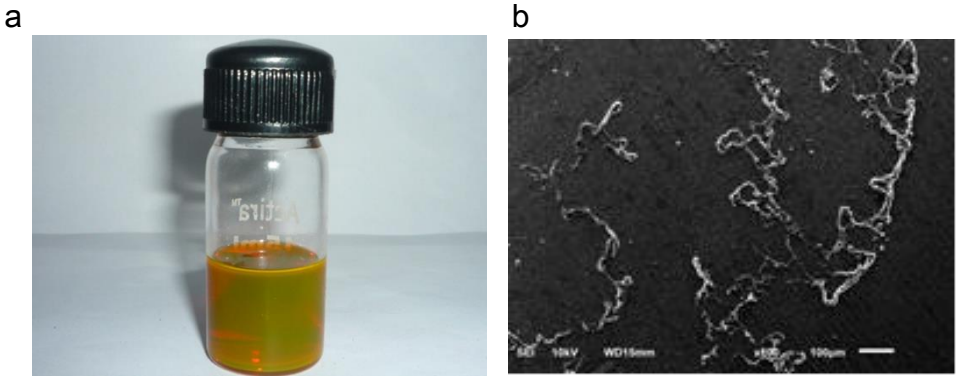

Figure 5. a) Self assembly image of BP-PTCDI obtained in MeOH/ $CHCl_3$ b) SEM image of the self-assembly of BP-PTCDI obtained in $CHCl_3$

3. RESULTS AND DISCUSSION

Self assembly of π conjugated systems such as PTCDIs is of immense interest in both academic and industrial areas owing due to their excellent properties and potential applications. They exhibit remarkable electronic properties and demonstrate high molar absorption coefficients in the visible region of the electromagnetic spectrum. Moreover, they are known to be thermally stable, and can form ordered nanostructures conducive to charge transport [**21**].

3.1. NMR studies

The 1D and 2D NMR data of compound **BP-PTCDI** are shown in **Tables 1 and 2** respectively.

Table1. ^{1}H and ^{13}C chemical shifts (ppm) for compound BP-PTCDI

Proton	^{1}H Chemical shift	^{13}C Chemical shift
1,3,8, 10	-	163.2
4,7,11,14	8.51 (d)	131.1
5,6,12,13	8.35 (d)	122.8
1′-1″	3.58 (t)	68.8
2′,2″	2.05 (m)	28.2
3′, 3″	4.30 (t)	38.4
5′, 5″	3.42 (t)	70.7
6′, 6″	1.48 (m)	31.8
7′, 7″	1.31 (m)	19.3
8′, 8″	0.84 (t)	13.9
Others (aromatic)	-	134.1
		129.1
		126.0
		123.1

From Fig 1, the perylene protons recorded as two doublets for BP-PTCDI were observed at a higher chemical shift of 8 ppm experimentally. The distribution of the protons is well spread as seen from the ^{1}H NMR spectrum. The methyl protons of the butyloxy groups appear as a triplet in the shielded region at 0.84 ppm corresponds to 6 hydrogens. In the ^{1}H-^{1}H COSY spectrum, these protons show cross peaks with the ^{1}H signal at 1.31 ppm (m) and the latter are assigned to H7′- H7″ methylene protons of the butyloxy moieties. These methylene protons show correlation with another multiplet at 1.48 ppm which is due to the resonance of H6′-H6″ methyl protons of the butyloxy group. A triplet at 3.42 ppm corresponding to the four hydrogens is assigned to H5′-H5″. Methylene protons based on their correlations with the proton signals are due to H6′-H6″.

Of the two triplets at 4.30 and 3.58 ppm, the deshielded one at 4.30 ppm is assigned to H3′ and H3″ methylene protons as they exhibit correlation with the multiplet 2.05 assignable for H2′ and H2″ methylene protons. Likewise the signal at 3.58 ppm is assigned to H1′ and H1″ protons attached to the imide nitrogen atoms in line with their correlation in the ^{1}H-^{1}H COSY spectrum.

Table 2. ^{1}H-^{1}H COSY and ^{1}H-^{13}C COSY CORRELATIONS for compound BP-PTCDI

^{1}H chemical shift	Correlations in ^{1}H-^{1}H COSY	Correlations in ^{1}H-^{13}C COSY
8.51 (d) (H4, H7, H11, H14)	8.35 (d)	131.1
8.35 (d) (H5, H6, H12, H13)	8.51 (d)	122.8
3.58 (t) (H1′, H1″)	2.05 (m)	68.8
2.05 (m) (H2′, H2″)	3.58 (t), 4.30 (t)	28.2
4.30 (t) (H3′, H3″)	2.05 (m)	38.4
3.42 (t) (H5′, H5″)	1.48 (m)	70.7
1.48 (m) (H6′, H6″)	1.31 (m), 3.42 (t)	31.8
1.31 (m) (H7′, H7″)	1.48 (m), 0.84 (t)	19.3
0.84 (t) (H8′, H8″)	1.31 (m)	13.9

In the aromatic regions of the spectrum, the deshielded signal at 8.51 ppm (d) is attributed to the H4, H7, H11 and H14 hydrogens and the shielded signal at 8.35 ppm (d) is due to the H5, H6, H12 and H13 protons. These assignments are in accordance with their spectral correlations observed in the ^{1}H-^{1}H COSY spectrum.

3.1.2. ^{13}C NMR spectrum

In the ^{13}C NMR spectrum of the compound, the deshielded signal at 163.2 ppm is assigned to the carbonyl carbons (C1, C3, C8 and C10) of the imide moiety. The signals at 13.9, 19.3, 28.2, 31.8 and 38.4 ppm are assigned to C8′ & C8″, C7′ & C7″, C2′ & C2″, C6′ & C6″, C3′ & C3″ methylene carbons res based on the correlations observed in the ^{1}H-^{13}C COSY spectrum.

The deshielded signals around the signal of $CDCl_3$ at 70.7 and 68.8 ppm are assigned to C5′ & C5″ and C1′ & C1″ methylene carbons attached to negative oxygen and nitrogen atoms as per observed from the ^{1}H-^{13}C COSY correlations. In the aromatic region of the spectrum, the resonance of C4, C7, C11 and C14 carbons are observed at 131.1 ppm. The signal of C5, C6, C12 and C13 carbons are observed at 122.8 ppm. The remaining quaternary carbons show their resonance between 123.1 and 134.1 ppm as less intense signals. These signals assignment of signals are in accordance with the observed ^{1}H-^{13}C COSY correlations.

The aromatic perylene ring clearly existed as two doublets at a higher chemical shift of 8 ppm experimentally. ^{13}C NMR spectrum showed the presence of carbonyl carbon at 163.2 ppm **(Fig S1)**. Signals at 134.1 to 131.1 ppm indicated the presence of aromatic carbons of the perylene and benzyl rings. From **Fig.2**, it can be implied that due to π-stacking interactions, the chemical shifts of the

perylene protons are highly shielded in the NMR diagram. The recorded ^{13}C, 2D NMR (^{1}H-^{1}H, ^{1}H-^{13}C) spectra of BP-PTCDI are given in **Fig S1 to S3 (Supplementary data).**

3.2. Optical studies

PTCDIs show strong absorption band in the visble region [**22**]. Kazmaier *et al.* reported that the PTCDIs, which exhibited larger valence and conduction band broadened by aggregation were also those with the higher photosensitvities [23]. In this work, we have carried out the UV-vis absorption spectral studies of **BP-PTCDI** in chloroform at various concentrations and are shown in **Fig.3a.** Compound **BP-PTCDI** showed monomeric π-π transition bands with three well defined peaks at 525, 488 and 459 nm

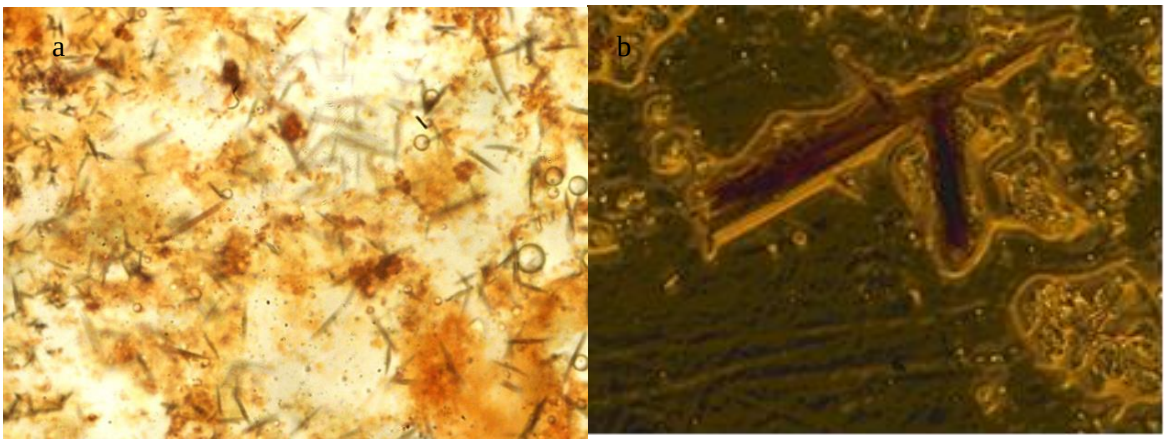

Figure 6. a) Optical microscopic images of the self-assembly of BP-PTCDI obtained in CHCl3 b) Fluorescence microscopic image of the self-assembly of BP-PTCDI obtained in CHCl3

marked as 0-0, 0-1 and 0-2 vibrational coupled electronic transitions of perylene diimide core in the monomeric state [24]. The maximum absorbing wavelength (λ_{max}) did not shift on changing the concentration. In simple words, we can say that the position of the maxima remained unaffected by the change in alkyl chain length of the substituent. However the observed bands were reminiscent with the absorption band of pure perylene and correspond to the $S_0 \rightarrow S_1$ transition and the dipole moment were directed parallel to the long axis of the molecule [**25, 26**].

In their studies, Kaur *et al.* mentioned that the introduction of both N-alkyl and N-aryl substituents have a minor effect on the charges of the diimide groups. And hence, the conformations and charge distributions of the terminal substituents are found to play a very important factor in determining the dipole moment of these molecules [**27**].

Mizuguchi *et al.* too reported that the resonance interactions of transition dipoles are responsible for the band splitting of the absorptions that appeared in perylene diimide (PDI) films [**28**].

The fluorescence spectra of the compound in chloroform at varied concentrations (λ_{max} = 460 nm) are shown in **Fig.3b.** Emission spectra are known to be more sensitive compared to the absorption spectra [**29**]. The emission peaks for compound **BP-PTCDI** appeared at 534 and 576 nm respectively. From the fluorescence figures, we observe that the fluorescence spectrum is a mirror image of the

absorption spectrum [**30**]. Since the two nitrogen positions of the diimides are at node of the π-orbitals [**31**], it can be seen that the substitution of the side chain does not change the electronic structure of the PTCDI molecule. Photon absorption in organic materials usually leads to the formation of a Frenkel exciton [32]. The formation of weak absorption bands at longer wavelength implies the weak or distorted π-π interaction in the aggregates.

3.3. Thermal studies

Differential scanning calorimetry (DSC) technique was used to study the morphological behaviour of compound **BP-PTCDI** under nitrogen atmosphere (heating rate 5 K min^{-1}) and is shown in **(Fig.4)**. The DSC thermogram of BP-PTCDI exhibited no glass transition temperature (T_g) during the DSC run (heating) up to 300°C. Compound BP-PTCDI with increasing temperature showed two endothermic peaks at ~ 80°C and 130°C. The first peak is due to the transition and second as the melting peak.

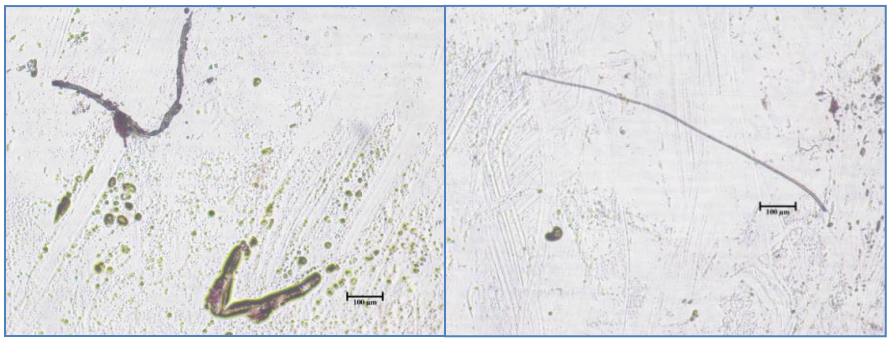

Figure 7. Phase contrast microscopic images of the self-assembly of BP-PTCDI obtained in $CHCl_3$

3.4. Self-assembly

Molecular level self-assembly includes supramolecular interactions for example hydrophobic and hydrophilic effects, electrostatic interactions, hydrogen bonding, micro phase segregation, and shape effects etc [33-36]. But it also makes use of kinetically labile covalent bonds [37-38]. Self-assembly formation can be performed by various techniques such as the solution-based self-assembly method, rapid solution dispersion method, phase transfer method, vapour diffusion technique, seeded growth, sol-gel processing technique, surface-supported self-assembly method and so forth [39,40]. In our work, we have used the conventional method in which the self-assembly of the molecule occurs at the interface between a poor (methanol) and rich (chloroform) solvent [41]. Such a technique has the advantage of strong intermolecular π-π interaction, which is enhanced in a solvent where the molecule has minimum interactions. The self-assembly of synthesized compounds in solution phase as well as at surfaces and interfaces are found to be difficult as they are largely dependent on kinetics and thermodynamics. Kinetics and thermodynamic studies are known to play a key role in the nucleation process [42,43].

But then organic semiconductors, especially those capable of forming crystalline nano/microstructures by solution-based self-assembly, have developed greatly and rapidly [44]. From literature studies, we observe that by increasing the alkyl chain length at the imide position helps to decrease the intermolecular aggregation of the perylene core by the decrease in the π-π stacking [**42**]. Long alkyl chains are known to import hydrophobic, steric and electronic interference during the self-assembling process which in turn are known to affect the nature of the self-assembly [45]. This can be attributed to the side chain of PTCDI which plays a majo rrole in controlling the molecular packing. Changes in the side chain are known to affect the colour and other physico-chemical properties of the PTCDI aggregates [46]. Substitution at the perylene core can bring about a deformation from planarity which causes hypsochromic shifts [**47**].

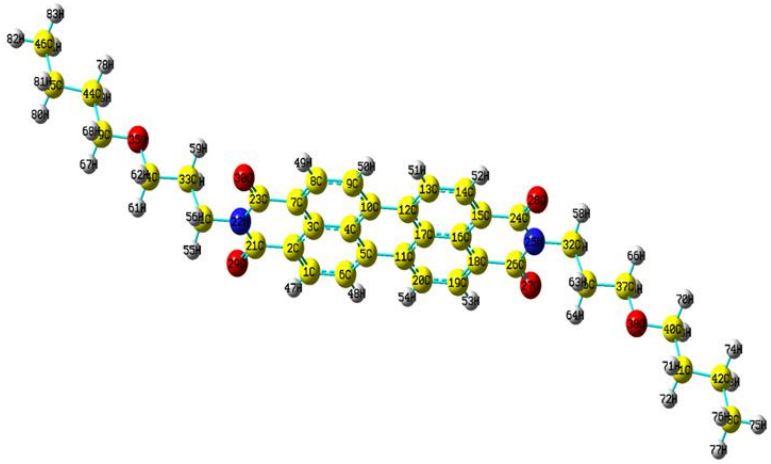

Figure 8. Optimized molecular structure of BP-PTCDI

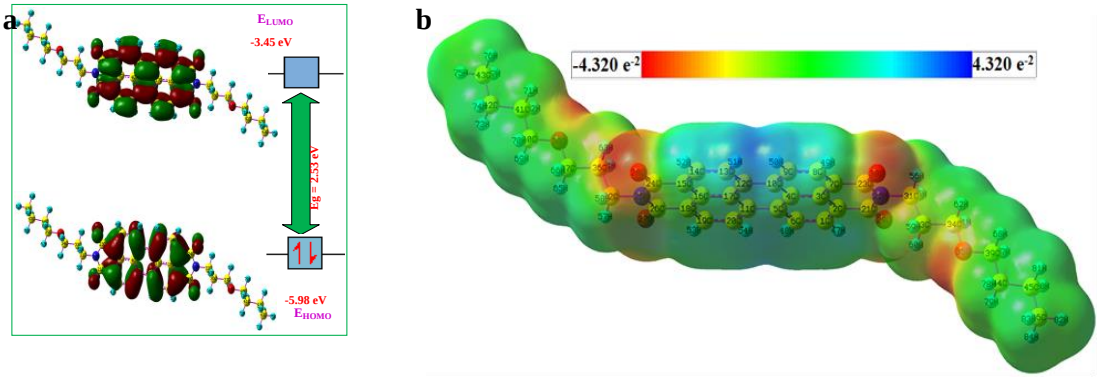

c

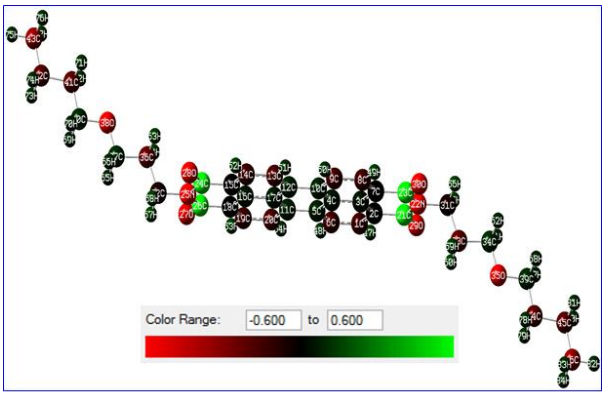

Figure 9. a) HOMO-LUMO energy gaps of BP-PTCDI b) Molecular electrostatic potential (MEP) image of BP-PTCDI c) Mulliken population analysis of BP-PTCDI

Also, self- assembly play a very important role in the formation and development of highly well ordered structures and also their helicity [42]. The formation of aggregates of compound **BP-PTCDI** is displayed in **Fig.5a**. The SEM image of the molecular assembly drop-casted onto a clean glass slide showed a chain like structure as seen in **Fig.5b**. The optical microscopic image revealed the formation of molecular rods as shown in (**Fig.6a)**. Dark brown emission was clearly observed from fluorescence microscopy **Fig.**6b. Phase contrast microscopy images **(Fig.7)** exhibited varying rod like morphologies such as bright red molecular rods/bundles, small short red rods, thin and long black rods, small short red and green rods, V-shaped rods. The short formed molecular rod and aggregates were found to be consistent with the distorted π-π stacking, which prevents the molecules from assembling along one dimension [6]. Thus the electronic properties of the organic materials depend upon the morphology and supramolecular packing [48].

3.5. Computational details

A complete computational study for the synthesized compound were performed with B3LYP/6–31G (*d,p*) as a basis set using Gaussian 09W [**49**] program package. Images were visualized using the GaussView 5.0 visualization program [**50**]. NBO calculations were carried out using NBO 3.1 program [**51**] as implemented in the Gaussian 09W. Optimized molecular structure for the synthesized compound BP-PTCDI is displayed in **Fig.8.**

3.5.1. HOMO-LUMO studies

PTCDI core is fairly electron deficient and thus easy to reduce and difficult to oxidize [52]. The planarity of the perylene core is generally affected by the introduction of long greater substituents at the bay position. A shift or a slight change in planarity can disturb the multi - dimensional electron transfer processes [53]. PTCDIs central core are usually held responsible for the π to π stacking and for the electronic structure of the material. It is generally known that the frontier molecular orbitals are in this region [13].

In our study, the optimized geometry of compound **BP-PTCDI** showed the presence of the HOMO and LUMO orbitals and is represented in **Fig.9a**. The frontier molecular orbitals are very useful for the characterization of organic compounds in both the ground and excited state. HOMO and LUMO calculations reveal the charge transfer within the molecule. Besides this the energy difference between the two orbitals is considered to be very important to determine the molecular electron transport properties. The energy gap values also helps to predict the global chemical reactivity descriptor of molecules such as hardness, chemical potential, softness, electronegativity and electrophilicity index as well as local reactivity have been determined [**54**]. The molecules which have a small energy gap are known as soft molecules, whereas molecules which have a large energy gap difference are referred to as hard molecules [**55**]. The ideal reason for performing the structural studies is to study the relationship between the optical properties and the structural modifications by using different substituents. **Fig.9a** show that the perylene (central) π system is the region where the π electrons are delocalized and which are influenced by the terminal substituents. This is indicated by the π-π transitions. The energy band gap values for compounds **BP-PTCDI** is found to be 2.53 eV respectively. The large band gap values indicate that this compound have strong intermolecular π-π interactions which in turn is responsible for their notable photochemical and photophysical stability, thereby making it suitable to be used as a suitable material in the application of organic electronics.

3.5.2. MEP analysis

Molecular electrostatic potential (MEP) deals with the study of electronic density and also helps to determine H-bonding interactions [**56**]. From **Fig.9b,** we can see that the core regions of the central aromatic region is positive as compared to the other regions. The red coloured region contains the oxygen atom and is found to influence the neighbouring atoms with yellow tinges. This observation also gives us a clear idea about the region from where the compound can undergo non-covalent interactions. Thus this method is found to be beneficial in elucidating the molecular structure of the synthesized compound.

3.5.3. Mulliken charge transfer

Mulliken population analysis is a powerful technique to investigate the charge transfer of quantified charges per atom in the molecules. In compound **BP-PTCDI**, the nitrogen and oxygen atoms are having negative charge due to more electro-negativity environment according to MEP. The oxygen bonded carbon atoms are only having more positive charge due to the charge transfer. The Mulliken charge transfer according to colour differentiation is represented in **Fig.9c**.

3.5.4. Natural bond orbital (NBO) analysis

NBO analysis is an efficient tool in elucidating the stereo electronic interactions on the reactivity and dynamic behavior of chemical compounds [**57**]. NBO helps us analyze the interactions between the intra and intermolecular bonding as well as provides a solid platform for investigating charge transfer or conjugative interactions in molecular system. In NBO analysis, the hyperconjugative σ→σ* interactions play a very important role. These interactions represent the weak departures from a strictly localized natural Lewis structure that constitutes the primary “non-covalent” effects. In compound **BP-PTCDI**, the strong intramolecular hyper conjugative interactions of π-electrons are derived as π (C1-C2) to π* (C21-

O29) is 22.35 kJmol^{-1}, π (C3-C4) to π* (C5-C6) is 18.18 kJmol^{-1}, π (C5-C6) to π* (C1-C2) is 20.48 kJmol^{-1}, π (C7-C8) to π* (C28- O30) is 22.35 kJmol^{-1}.

4. CONCLUSIONS

Here in this paper, a newly synthesized compound was studied for its UV-vis and fluorescence properties and its molecular geometry was optimized. It was found that the observed absorption and emission spectra of the synthesized compound **BP-PTCDI** were in accordance with respect to their readings. There was not much difference in their absorption or emission wavelength. HOMO-LUMO studies revealed that charge transfer does take place in the molecule. The Mulliken charge analysis also explains the confirmation of charge transfer of atoms in the molecule. MEP diagram reveal the difference between the chemically active and inactive sites and hence the reactivity of atoms can be compared. NBO studies revealed the stability of the molecules arising from hyper-conjugative interaction and charge delocalization. Thus from both experimental and theoretical studies, it can be confirmed that this compound is found to be suitable for potential applications in the organic electronic industry.

References

[1] Maryam. N; Synthesis of a Novel Fluorescent Optical pH Sensor, M.Sc Thesis from Eastern Mediterranean University, Gazimağusa, North Cyprus, **2011**.

[2] El-Nahhas. M., Abdel-Khalek. H., Salem. E., Optical Properties of 3,4,9,10-Perylenetetracarboxylic Diimide (PTCDI) Organic Thin Films as a Function of Post-Annealing Temperatures, *Am. J. Materials Sci*, **2012**, *2*, 131-137.

[3] El-Daly. SA; Salem. A; Hussein. MA; Asiri. AM; Fluorescence quenching N,N-bis(2,6-dimethylphenyl)-3,4:9,10-perylenetetracarboxylic diimide (BDPD) laser dye by colloidal silver nanoparticles, *J. Fluor*, **2015**, *25*, 379-85.

[4] Boobalan. G., Imran. P.K.M., Nagarajan. S., Luminescent one-dimensional nanostructures of perylene bisimides, Spectrochim. Acta, A., *Mol. Biomol Spectr*, **2013**, *113*, 340–345.

[5] Boobalan. G., Imran. P.K.M., Nagarajan. S., Synthesis of highly fluorescent and water soluble perylene bisimide, *Chin. Chem Ltrs*, **2012**, *23*, 149–153

[6] Boobalan. G., Imran. P.K.M., Nagarajan. S., Self-assembly, optical and electrical properties of fork-tailed perylene bisimides, *Superlattices Microstruct* **2012**, *51*, 921–932

[7] Boobalan. G., Imran. P.K.M., Ramkumar. S.G., Nagarajan. S., Fabrication of luminescent perylene bisimide nanorods, *J. Luminescence* **2014**, *146*: 387–393

[8] Boobalan. G., Imran. P.K.M., Ramkumar. S.G., Nagarajan. S., Fabrication of highly fluorescent perylene bisimide nanofibers through interfacial self-assembly, *J. Colloid. Interface Sci*, **2013**, *393*, 377–383

[9] Willy. H., Klaus Hunger Production, Properties, Applications Third, Completely Revised Edition,, Industrial Organic Pigments 3rd ed - W. herbst, K. Hunger (Wiley, **2004**) WW (1).

[10] Michael. R. R., Sambandam. A., Rajadurai. V. S., Ponnambalam V., Sundar K. I. S., Muthupandian. A., Synthesis of conjugated perylene diimide-based copolymer with 5,5 -bis(4-aminophenyl)-2-2 -bifuryl moiety as an active material for organic photovoltaics, *J. Photochem. Photobio A.*, **2012**, *247*, 52–62

[11] Schmidt. D., Bialas. D., and Wurthner. F., *Angew. Chem.* **2015**, 127 (12), 3682 –3685.

[12] Louisa. M. S., David. L., Adam. B. B. W., and John. A. M., Kinetics of Charge Trap Formation in n-Channel Semiconductors Studied by Time- and Wavelength-Resolved Electric Force Microscopy, *ISDRS* **2013**, December 11-13.

[13] Boobalan. G., Mohamed Imran. P., Nagarajan. S., Self-Assembly, Optical, and Electrical Properties of a Novel Water-Soluble Perylene Bisimide, *J. Electron. Mater.*, **2011**, *40*, 2392-2397.

[14] Arantes. J. T., Lima. M. P., Fazzio. A., Xiang. H., Su-Huai W., and Dalpian. G. M., J. Effects of Side-Chain and Electron Exchange Correlation on the Band Structure of Perylene Diimide Liquid Crystals: A Density Functional Study, *Phys. Chem. B* **2009**, *113*, 5376–5380.

[15] Junxiang. Z., Sanjeev. S., Do. K. H., Stephen. B., Bernard. K., and Seth. R. M., Self-assembly of a set of hydrophilic–solvophobic–hydrophobic coil–rod–coil molecules based on perylene diimide, *Phys. Chem. Chem. Phys.*, **2013**, *15*, 21058-21069.

[16] Gesche. R., and Sigurd. H. G., N-Alkylated and N,N-dialkylated 1,6-diaminoperylene diimides synthesized via copper catalyzed direct aromatic amination, *Chem. Commun*., **2014**, *50*, 5659.

[17] Molla R. I., and Sundararajan. P. R., 1,6- and 1,7-Regioisomers of Asymmetric and Symmetric Perylene Bisimides: Synthesis, Characterization and Optical Properties, *Molecules*, **2014**, *19*: 327-341.

[18] Horowitz, G.; Kouki, F.; Spearman, P.; Fischou, D.; Nogues, C.; Pan, X.; Garnier, F. Evidence for n-type conduction in a perylene tetracarboxylic diimide derivative, *Adv. Mater* **1996**, 8: 242-244

[19] Tasch, S.; List, E. J. W.; Hochfilzer, C.; Leising, G.; Rohr, U.; Schlichting, P.; Geerst, Y.; Scherft, A.; Müllen, K. Efficient red- and orange-light-emitting diodes realized by excitation energy transfer from blue-light-emitting conjugated polymers, *Phys. Rev. B* **1997**, 56: 4479

[20] Aamer. S., Ghulam. S., New fluorescent symmetrically substituted perylene-3,4,9,10-dianhydride-azohybrid dyes: Synthesis and spectroscopic studies, *Spectrochim. Acta, Part A: Mol.Biomol Spectr*, **2014**, 133: 7–12

[21] Baysec S., Akbasoglu Unlu N., Hacioglu S. O., Arslan Udum Y., Cirpan A. & Toppare L., Electrochemical Properties of Perylene Diimide (PDI) and Benzotriazole (Btz) Bearing Conjugated Polymers to Investigate the Effect of π-Bridge on Electrochemical Properties, *J. Macromol. Sci., Pure Appl. Chem*., **2015**, 52: 1–9

[22] Andrew. J. T., Chang. G., Mark. B. M., Tyler. B. S., Han. Y., Yuning L., Dwight. S. S., Thionation Enhances the Electron Mobility of Perylene Diimide for High Performance n-Channel Organic Field Effect Transistors, *Adv. Funct. Mater*. **2015**, 25, 3321-3329

[23] Xin. Z., Zhenhuan. L., Long. Y., Chuanlang. Z., Jianhui. H., Shaoqing. Z., Bo. J., Yan. Z., Jianhua. H., Shanlin. Z., Yang. L., Qiang. S., Yunqi. L., and Jiannian. Y., *Adv. Mater*. **2013**, *25*: 5791–5797

[24] Kazmaier P. M., Hoffmann R., A Theoretical Study of Crystallochromy. Quantum Interference Effects in the Spectra of Perylene Pigments, *J. Am. Chem. Soc*. **1994**, 116: 9684

[25] Wurthner F., Bauer C., Stepanenko V., Yagai S., A Black Perylene Bisimide Super Gelator with an Unexpected J-Type Absorption Band, *Adv. Mater*., **2008**, 20: 1695

[26] Shi M.M., Chen H.Z., Shi Y. W., Sun J.Z., Wang M., Unique Aggregate Structure of Fluoroperylene Diimide Thin Film, *J. Phys. Chem. B*, **2004**, 108: 5901.

[27] Thulstrup E.W, Michl., J., Eggers J.H., Polarization spectra in stretched polymer sheets. II. Separation of π-.π absorption of symmetrical molecules into components, *J. Phys. Chem*., **1970**, 74: 3868

[28] Balwinder. K., Sati N. B., David. J. H., Interpreting the near-infrared reflectance of a series of perylene pigments, *Dyes and Pigments*, **2013**, 99, 502-511.

[29] Mizuguchi, J.; Tojo, K. Electronic Structure of Perylene Pigments as Viewed from the Crystal Structure and Excitonic Interactions, *J. Phys. Chem. B* **2002**, *106*: 767-772

[30] Feng J., Liang B., Wang D., Wu H., Xue L., Li X., Synthesis and Aggregation Behavior of Perylenetetracarboxylic Diimide Trimers with Different Substituents at Bay Positions, *Langmuir*, **2008**, 24: 11209-11215

[31] Liu S.G., Sui G., Cormier R. A., Leblanc R. M., Brian A. Gregg, Self-Organizing Liquid Crystal Perylene Diimide Thin Films: Spectroscopy, Crystallinity, and Molecular Orientation, *J. Phys. Chem. B*, **2002**, 106: 1307-1315.

[32] Langhals H., Cyclic Carboxylic Imide Structures as Structure Elements of High Stability. Novel Developments in Perylene Dye Chemistry, *Heterocycles*, **1995**, 40: 477-500

[33] Lifshitz E., Kalpana A., Ehrenfreund E., Meissner D., Optically detected magnetic resonance as a tool to study the morphology of perylene-derivative thin film, *Chem.Phy.Lett*. **1999**, 300, 626-632.

[34] Narayan B., Senanayak S. P., Jain A., Narayan K. S., George S. J., Self-Assembly of π-Conjugated Amphiphiles: Free Standing, Ordered Sheets with Enhanced Mobility, *Adv. Funct. Mater*., **2013**, 23: 3053-3060.

[35] Rao K. V., Jayaramulu K., Maji T. K., George S. J., Supramolecular Hydrogels and High-Aspect-Ratio Nanofibers through Charge-Transfer-Induced Alternate Coassembly, *Angew. Chem. Int. Ed.*, **2010**, 49: 4218-4222

[36] Rao V., George S. J., Synthesis and Controllable Self-Assembly of a Novel Coronene Bisimide Amphiphile, *Org. Lett.*, **2010**, 12: 2656–2659.

[37] Zhang X., Rehm S., Safont-Sempere M. M., Würthner F., Vesicular perylene dye nanocapsules as supramolecular fluorescent pH sensor systems, *Nat. Chem*., **2009**, 1: 623-629.

[38] Dhotel A., Chen Z., Delbreilh L., Youssef B., Saiter J.-M., Tan L., Molecular Motions in Functional Self-Assembled Nanostructures, *Int. J. Mol. Sci*. **2013**, 14: 2303-2333.

[39] Busseron E., Ruff Y., Moulin E., Giuseppone N,, Supramolecular self-assemblies as functional nanomaterials, *Nanoscale*, **2013**, 5: 7098-7140.

[40] Zhang L., Che Y., Moore J. S., One-Dimensional Self-Assembly of Planar π-Conjugated Molecules: Adaptable Building Blocks for Organic Nanodevices, *Acc. Chem. Res*., **2008**, 41: 1596-1608.

[41] Guo Y., Xu L., Liu H., Li Y., Che C.-M., Li Y., Self-Assembly of Functional Molecules into 1D Crystalline Nanostructures, *Adv. Mater*., **2015**, 27: 985-1013.

[42] Che Z. Y., Moore J.S., One-dimensional self-assembly of planar pi-conjugated molecules: adaptable building blocks for organic nanodevices, *Acc. Chem. Res*., **2008**, 41: 1596

[43] Hu J., Kuang W., Deng K., Zou W., Huang Y., We Z., F.J. Faul, Self-Assembled Sugar-Substituted Perylene Diimide Nanostructures with Homochirality and High Gas Sensitivity, *Adv. Funct. Mater*., **2012**, 22: 4149-4158

[44] Okamoto K., Chithra P., Richards G. J., Hill J. P., Ariga K., Self-Assembly of Optical Molecules with Supramolecular Concepts, *Int. J. Mol. Sci*. **2009**, 10: 1950-1966

[45] Mukherjee B., Sim K., Shin T. J., Lee J., Mukherjee M., Reec M., Pyo S., Organic phototransistors based on solution grown, ordered single crystalline arrays of a π-conjugated molecule, *J. Mater. Chem*., **2012**, 22: 3192.

[46] Murugavelu M., Imran P.K.M., Sankaran K.R., Nagarajan S., Self-assembly and photophysical properties of a minuscule tailed perylene bisimide, *Mater. Sci.Semicond. Process.* **2013**, 16: 461-466

[47] Boobalan G., Imran P.K.M., Nagarajan S., *Spectrochim.Acta, Part A: Mol.Biomol.Spectrosc.*, **2013**, 113: 340-345

[48] Nisha. V. H., Laura. D. S., Barry. K. L, Douglas. R. P., and Darrell. B. K., Phosphorus, 1,6- And 1,7-Regioisomers of Perylene Tetracarboxylic Dianhydride and Diimide: The Effects of Neutral Bay Substituents on the Electrochemical and Structural Properties, *Phosphorus, Sulfur Silicon Relat. Elem*, **2014**, 189: 738–752.

[49] Simone Fabiano, He Wang, Claudia Piliego, Cherno Jaye, Daniel A. Fischer, Zhihua Chen, Bruno Pignataro, Antonio Facchetti, Yueh-Lin Loo, and Maria Antonietta Loi *Adv. Funct. Mater*. **2011**, 21: 4497-4486

[50] Frisch M. J. *et al*., Gaussian-09, Revision A.01, Gaussian, Inc., Wallingford, CT **2009**.

[51] Dennington R., Keith T., and Millam J., GaussView, Version 5, Semichem Inc., Shawnee Mission KS. **2009**.

[52] Reed A. E., Curtiss L. A., and Weinhold F., Intermolecular interactions from a natural bond orbital, donor-acceptor viewpoint, *Chem. Rev*. **1988**, 88: 899

[53] Mahuya. B., Tanmoy. D., Haizhen. Z., Shaohua. L., Sanjiban. C., Andrew. K., Zhonghua. P., Synthesis and optical properties of perylene diimide derivatives with triphenylene-based dendrons linked at the bay positions through a conjugated ethynyl linkage, *Tetrahedron*, **2012**, 68, 2806-2818

[54] Dinçalp, H., Çimen. O., Ameri. T., Brabec. C.J., İçli. S., Synthesis, characterization and optoelectronic properties of a new perylene diimide–benzimidazole type solar light harvesting dye, *Spectrochim. Acta A., Mol.Biomol Spectr*, **2014**, 128: 197–206

[55] Sheela N.R., Sampathkrishnan S., Thirumalai Kumar M., Muthu S., Quantum mechanical study of the structure and spectroscopic, first order hyperpolarizability, Fukui function, NBO, normal coordinate analysis of Phenyl-N-(4-Methyl Phenyl) Nitrone, *Spectrochim. Acta Part A: Mol.Biomol Spectr*, **2013**, 112: 62–77

[56] Moghanian H., Mobinikhaledi A., Monjezi R., Synthesis, spectroscopy (vibrational, NMR and UV–vis) studies, HOMO–LUMO and NBO analysis of 8-formyl-7-hydroxy-4-methylcoumarin by ab initio calculations, *J.Mol Struct*, **2013**, 1052, 135–145.

[57] Aditya Prasad A., Meenakshisundaram S P., Crystal growth, characterization and Density functional theory computations of supramolecular N-carbamothioyl acetamide *Cryst. Res. Technol*, 50, **2015**, No. 5, 395–404

[58] Pir H., Günay N., Tamer Ö., Avcı D., Atalay Y., Theoretical investigation of 5-(2-Acetoxyethyl)-6-methylpyrimidin-2, 4-dione: Conformational study, NBO and NLO analysis, molecular structure and NMR spectra, *Spectrochim. Acta Part A: Mol. Biomol Spectr*, **2013**, 112: 331–342

The authors declare no conflict of interest